scientific reports

Check for updates

OPEN

Selective etching of silicon nitride over silicon oxide using ClF_3/H_2 remote plasma

Won Oh Lee[1,5], Ki Hyun Kim[1,5], Doo San Kim[1], You Jin Ji[1], Ji Eun Kang[1], Hyun Woo Tak[1], Jin Woo Park[1], Han Dock Song[2], Ki Seok Kim[3], Byeong Ok Cho[2], Young Lae Kim[2] & Geun Young Yeom[1,4]✉

Precise and selective removal of silicon nitride (SiN_x) over silicon oxide (SiO_y) in a oxide/nitride stack is crucial for a current three dimensional NOT-AND type flash memory fabrication process. In this study, fast and selective isotropic etching of SiN_x over SiO_y has been investigated using a ClF_3/H_2 remote plasma in an inductively coupled plasma system. The SiN_x etch rate over 80 nm/min with the etch selectivity (SiN_x over SiO_y) of ~ 130 was observed under a ClF_3 remote plasma at a room temperature. Furthermore, the addition of H_2 to the ClF_3 resulted in an increase of etching selectivity over 200 while lowering the etch rate of both oxide and nitride due to the reduction of F radicals in the plasma. The time dependent-etch characteristics of ClF_3, ClF_3 & H_2 remote plasma showed little loading effect during the etching of silicon nitride on oxide/nitride stack wafer with similar etch rate with that of blank nitride wafer.

As the semiconductor device size is decreased to sub-nanoscale and the device integration is changed from two dimensional to three dimensional structure, more precise and selective etch technology is required for the semiconductor device fabrication[1]. In the various semiconductor devices, silicon nitride has been widely used as a barrier layer for dopant diffusion, a gate sidewall spacer layer, a buffer layer, etc. due to high insulating characteristics, high thermal and mechanical stability, etc. and selective etching of silicon nitride over silicon and/or silicon oxide is important for various microelectronic applications[2].

These days, in the three dimensional NOT-AND type flash memory fabrication, the number of silicon nitride/silicon oxide (SiN_x/SiO_y) stack is increasing and the thickness of repeating SiN_x/SiO_y layer is decreasing continuously for higher memory density in the vertical direction. Therefore, the etching of SiN_x layers uniformly and ultra-high selectively to SiO_y layers in the SiN_x/SiO_y stack is becoming more challenging process. Until now, the selective etching of SiN_x in SiN_x/SiO_y stacks is achieved by wet etching using a hot phosphoric acid (H_3PO_4)[3–6]. In case of the wet etching, however, the penetration of an etch solution into holes is getting more challenging as the thickness of the SiN_x/SiO_y layer is decreased and the remaining SiO_y layers can be collapsed due to the surface tension. Moreover, several additives for increasing the etch selectivity of SiN_x/SiO_y are found to cause oxide regrowth problems after etching unless its process condition is not carefully controlled[5]. To solve these problems, a dry process for isotropic and selective etching of SiN_x needs to be developed as an alternative technology for three dimensional NOT-AND type flash memory fabrication.

Various studies have been reported for selective etching of SiN_x over SiO_y using dry etch processes. For example, an ultra-high selective etching of SiN_x over SiO_y was reported using CF_4-based ($CF_4/O_2/N_2$, CF_4/CH_4/Ar) gases with a microwave chemical downstream etcher and an inductively coupled plasma (ICP) etcher[7–9]. In addition, NF_3-based ($NF_3/O_2/NH_3$, $NF_3/O_2/N_2$) gases were also used to ultra-high selective etching of silicon nitride over silicon oxide with downstream etchers based on ICP or capacitively coupled plasma (CCP)[9–13]. However, the etch selectivity of nitride over oxide still needs to be increased further for the application of current semiconductor process due to the thin thickness of oxide. Moreover, the use of fluorocarbon (CF_x) etch gases has contamination issues by carbon or deposition of CF_x (CH_x) polymers on the surface of the film, and which is a detrimental factor for a device fabrication. Even though these limits for engineering aspects are excluded,

[1]School of Advanced Materials Science and Engineering, Sungkyunkwan University, 2066 Seobu-ro, Jangan-gu, Suwon-si, Gyeonggi-do 16419, Republic of Korea. [2]Research and Development Group, Wonik Materials Co. Ltd., Cheongju 28125, Republic of Korea. [3]Research Laboratory of Electronics, Massachusetts Institute of Technology, Cambridge, MA, USA. [4]SKKU Advanced Institute of Nano Technology (SAINT), Sungkyunkwan University, 2066 Seobu-ro, Jangan-gu, Suwon-si, Gyeonggi-do 16419, Republic of Korea. [5]These authors contributed equally: Won Oh Lee and Ki Hyun Kim. ✉email: gyyeom@skku.edu

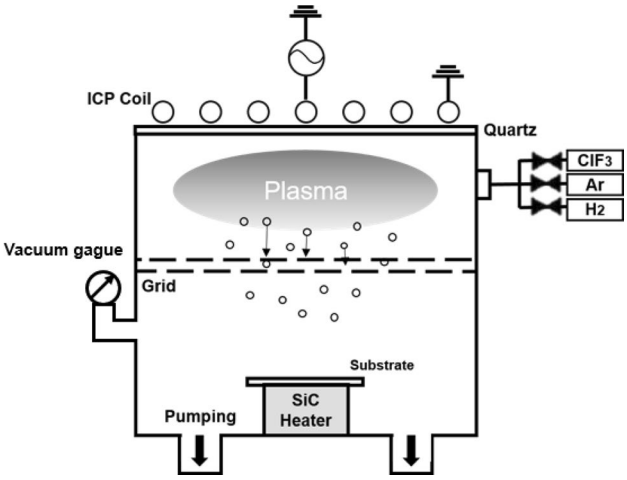

Figure 1. Schematic drawing of a remote-type inductively coupled plasma (ICP) etcher. At the center of the chamber, double grids having multiple holes are installed to prevent an ion bombardment and to deliver radicals only to the substrate. During the process, the substrate temperature was controlled (RT ~ 500 °C) by a silicon carbide (SiC) heater located below the substrate.

the high global warming potentials (GWPs) of CF_4- and NF_3-based etch gases [GWP values; CF_4 (7,390), NF_3 (17,200)] arouse the needs for the alternative etch gases for environmental aspects in the near future[14].

ClF_3 with the GWP of ~ 0 has been used primarily as an in-situ cleaning gas for chemical vapor deposition (CVD) chambers in replacement of perfluorocarbon compounds (PFC), which have high GWP values or as an etch gas for silicon etching by heating, neutral cluster beam etching, reactive ion beam etching, etc.[15–19]. In addition, the ClF_3 have been investigated for etching of SiGe in an ICP system[20], SiC etching with ultra-high etch rate over 10 μm/min[21], selective etching of transition metals and metal nitrides such as tantalum (tantalum nitride) over metal oxide (Ta_2O_5) with low pressure gaseous etching method[22]. In this study, ClF_3 remote plasma was applied for a fast and ultra-high selective etching of silicon nitride (SiN_x) over silicon oxide (SiO_y) applicable for current and next-generation semiconductor device fabrication including three dimensional NOT-AND type flash memory. The etching of SiN_x using ClF_3 showed high etch rate over 80 nm/min and the etch selectivity of SiN_x over SiO_y of ~ 130. The etch selectivity of SiN_x was further increased with H_2 addition in the ClF_3 plasma. The effect of Cl, F, and H radicals on the selective etching of SiN_x was investigated using plasma and surface analysis tools, and its etch mechanism was suggested.

Experimental section

Etching of silicon nitride. Figure 1 is a schematic drawing of a remote type inductively coupled plasma (ICP) etching system used in this study. The inside of process chamber was coated with an aluminum oxide layer by anodizing. The base pressure of the process chamber measured with a convection gauge was maintained at 3×10^{-3} Torr and the operating pressure monitored by capacitance manometer (Baratron gauge) was maintained at 200 mTorr. 13.56 MHz RF power was applied to the planar type ICP coil at upper side of a chamber. For the isotropic etching of SiN_x, double grids with multiple holes with 1.5 mm radius were arranged at the center of ICP reactor to prevent an ion bombardment effect and deliver radicals on the substrate. The substrate temperature was measured at the sample stage below the sample, which was monitored by a thermocouple and adjusted from 25 to 500 °C by a silicon carbide (SiC) heater connected to an external power supply. The chlorine trifluoride (ClF_3, > 99.9%, 200 sccm), H_2 (> 99.999%), and Argon (> 99.999% Ar, 200 sccm) were flown through a circular shape gas distributor to the process chamber.

Sample preparation. Blank 1.5 μm thick SiN_x thin films, blank 300 nm thick SiO_y thin films, and multilayer stacks composed of repeating SiO_y (27 nm) and SiN_x (27 nm) thin films were deposited by a plasma enhanced chemical vapor deposition (PECVD) process (supplied by WONIK IPS Inc.).

Characterization. The etch rate of SiN_x and SiO_y were measured by a step profilometer (Tencor, Alpha-step 500) and with Scanning Emission Microscopy (SEM, Hitachi S-4700) after patterning with photoresist (PR, AZ 5214E) as an etch mask. Also, the etch profiles of the multilayer thin films composed of SiN_x/SiO_y stacks were observed by the SEM. The surface roughness of films after the etching was measured by atomic force microscope (AFM, XE-100, Park System) with a non-contact measurement mode. The characteristics of ClF_3/H_2 plasma were analyzed with Optical Emission Spectrometry (OES, Avaspec-3648). Byproduct gases during etching process were monitored with Fourier-Transform Infrared Spectroscopy (FT-IR, MIDAC 12,000). The binding state and atomic composition of SiN_x and SiO_y (thin films of initial thickness of 500, 300 nm, respectively) before and after the etching were analyzed by X-ray Photoelectron Spectroscopy (XPS, MXP10, ThermoFisher Scientific) with a monochromated Al Kα source (1,486.6 eV) with spot size of 400 μm. The expected energy resolution of XPS is below 0.5 eV FWHM. The Avantage 5.0 software was used for curve fittings and the areas of each peak

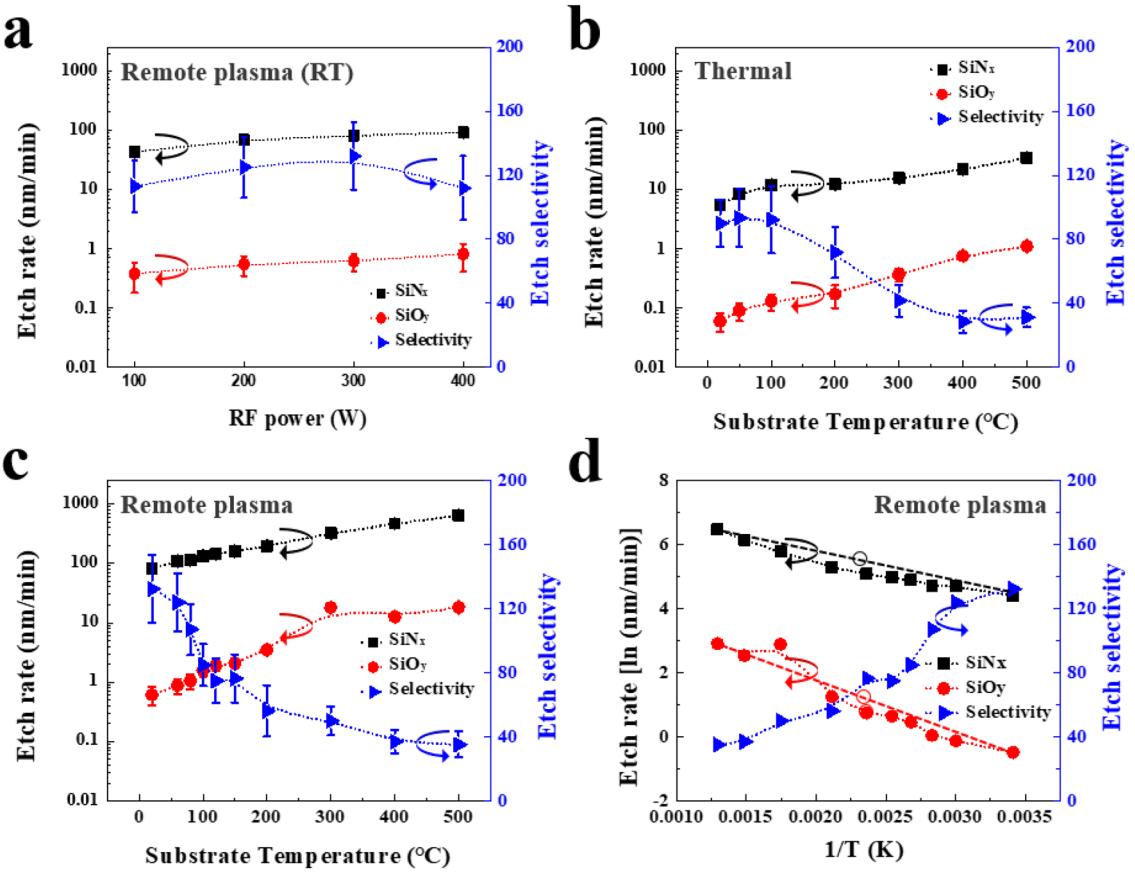

Figure 2. Etch characteristics of SiN_x and SiO_y (**a**) as a function of rf power for ClF_3 remote plasma at RT, (**b**) as a function of substrate temperature for chemical etching with ClF_3 gas flow only, and (**c**) as a function of substrate temperature for ClF_3 remote plasma at 300 W of rf power. 200 sccm Ar (200 sccm) was added to ClF_3 for plasma stability. (**d**) logarithm etch rates versus 1/T for ClF_3 remote plasma etching of SiN_x and SiO_y in (**c**) for the extraction of the activation energies.

were calculated with shirley background. The incident angle of X-ray to the sample was 50° and a hemispherical sector energy analyzer was positioned perpendicular to the sample stage.

Results and discussion

Figure 2 shows etch characteristics of SiN_x and SiO_y with ClF_3 gas only and ClF_3 remote plasmas. For ClF_3 remote plasmas, 200 sccm of Ar was added to 200 sccm of ClF_3 for the plasma stability. As shown in Fig. 2a, the etch rates of SiN_x and SiO_y were increased gradually with increasing rf power due to the enhanced dissociation of ClF_3 reaching the maximum etch rates of SiN_x and SiO_y at ~ 90 and ~ 0.8 nm/min, respectively. Note that, the etch selectivity of SiN_x over SiO_y didn't vary significantly (~ 120) over rf powers of 100 ~ 400 W. As shown in Fig. 2b, the SiN_x and SiO_y could be also etched just by flowing ClF_3 gas only without dissociating ClF_3 by rf plasmas and the increase of substrate temperature increased the etch rates of both films. However, the overall SiN_x etch rates by ClF_3 gas flow only were much lower compared to etching with ClF_3 remote plasmas, and which demonstrates that ClF_3 remote plasma etching is much more effective method for SiN_x etching compared with that by thermal etching without plasma. Meanwhile, even though etch rates of both materials were increased with increasing the substrate temperature, the etch selectivity of SiN_x over SiO_y was decreased. Same trend was observed for remote plasma etching. As shown in Fig. 2c, the increase of substrate temperature to ~ 500 °C at a fixed rf power of 300 W showed a gradual decreases of etch selectivity below 40 while showing increased SiN_x etch rates over 600 nm/min. The effect of process temperature on the etching of SiN_x and SiO_y can be understood by plotting the etch rates of SiN_x and SiO_y logarithmically as a function of inverse temperature (1/T) for ClF_3 remote plasma etching as shown in Fig. 2d. For the chemically activated etching, the etch rates can be described as a following Arrhenius equation.

$$\ln k = -\frac{E_a}{R}\left(\frac{1}{T_2} - \frac{1}{T_1}\right)$$

where k is a rate constant, R is the gas constant (1.987 cal K^{-1} mol^{-1}), T is the process temperature (K), and E_a is the activation energy. The calculated activation energies (E_a) of SiN_x and SiO_y were 1.93 and 3.18 kcal/mole, respectively. The higher activation energy of SiO_y means that the etch rate of SiO_y rises faster than that of SiN_x with the increase of temperature, and which leads to the decreases in etch selectivity of SiN_x over SiO_y even

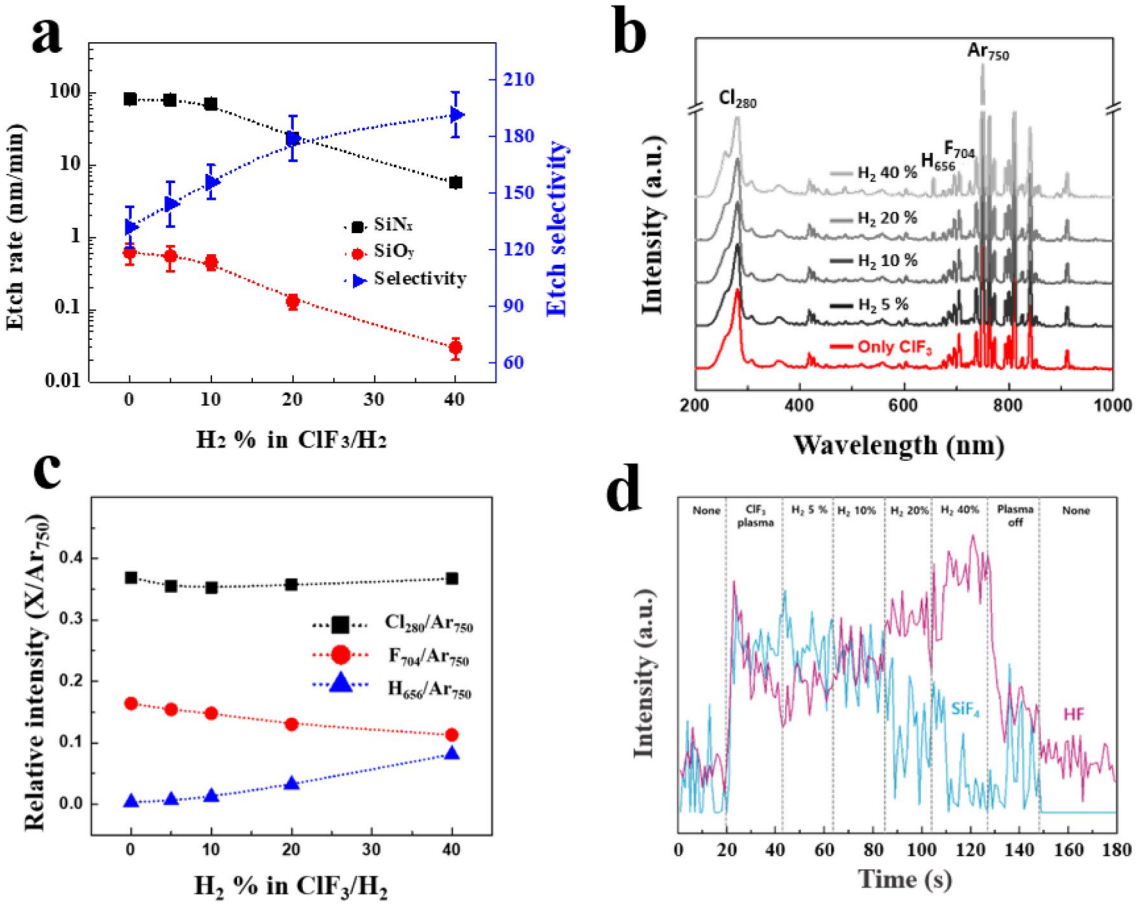

Figure 3. (**a**) Etch characteristics of SiN_x and SiO_y with ClF_3/H_2 plasma as a function of H_2 percentage in ClF_3/H_2. (**b**) OES data of $ClF_3/H_2/Ar$ plasma with different H_2 percentage in ClF_3/H_2. (**c**) optical emission intensities of Cl, F, and H normalized by the intensity of Ar (750 nm) in (**b**) plotted as a function of H_2 percentage. (**d**) FTIR data of ClF_3/H_2 plasma during SiN_x etching. For ClF_3/H_2 remote plasmas, 200 sccm of Ar was added for the plasma stability.

though the etch rates of both materials are increased exponentially with increasing substrate temperature. The root mean square (RMS) surface roughness of SiN_x and SiO_y after the etching with each process condition (remote plasma- and thermally-etching) showed no significant differences in the RMS surface roughness among the samples for different etch methods (Figure S1, supplementary information).

To improve the etch selectivity of SiN_x over SiO_y, H_2 was added to ClF_3 in addition to Ar (Ar was also added to ClF_3/H_2 for plasma stability) and, the effect of H_2 addition to ClF_3 on the etch characteristics of SiN_x and SiO_y was investigated as a function of H_2 percentage in ClF_3/H_2 ($ClF_3/H_2/Ar$ plasma) and the results are shown in Fig. 3a. To increase the H_2 percentage in ClF_3/H_2, H_2 flow rate was increased while keeping the substrate temperature at 25 °C, operating pressure at 200 mTorr, the ClF_3 flow rate at 200 sccm, Ar flow rate at 200 sccm, and the rf power at 300 W. The etch rates of both SiN_x and SiO_y were decreased with the increase of H_2 percentage, however, the etch selectivity of SiN_x over SiO_y was increased with the increase of H_2 percentage in ClF_3/H_2. To study the mechanism of selectivity SiN_x etching over SiO_y, the dissociated species in the plasmas was investigated by OES at the center of chamber and the byproducts during the process was monitored using FTIR at the pumping site. Figure 3b,c shows optical emission spectra and the relative emission peak intensities of Cl, F, and H normalized by the intensity of Ar as a function of H_2 percentage in ClF_3/H_2, respectively. In Fig. 3b, the optical emission peak intensities related to Cl, H, F, and Ar could be measured at 280, 656, 704, and 750 nm, respectively. In Fig. 3c, the optical emission intensities of Cl, F, and H were normalized by the optical emission intensity of Ar (750 nm) to minimize the effect of electron density on the estimation of radical density from the emission intensity. As shown in Fig. 3c, the increase of H_2 percentage did not change the intensity of Cl, however, it decreased F intensity while increasing H intensity. Figure 3 shows the FTIR data of the byproduct gases such as SiF_4 and HF measured at the pumping site for different H_2 percentage in ClF_3/H_2. As the flow rate of H_2 is increased, the concentration of SiF_4 was decreased, and which means that the etching of SiN_x was suppressed while increasing HF concentration due to the reaction of hydrogen (H) with fluorine (F) radical in the plasma. Usually, the addition of hydrogen to fluorine based plasma leads to scavenging of F radicals by forming gaseous HF molecules [23,24] which have negligible effects on the etching of SiN_x (and SiO_y) unlike their aqueous (ionized) state[25,26].

The Si binding states and surface composition of SiN_x and SiO_y after the ClF_3/H_2 plasma etching were analyzed using X-ray Photoelectron Spectroscopy (XPS) and the results are shown in Fig. 4 and Table 1. The SiN_x and SiO_y

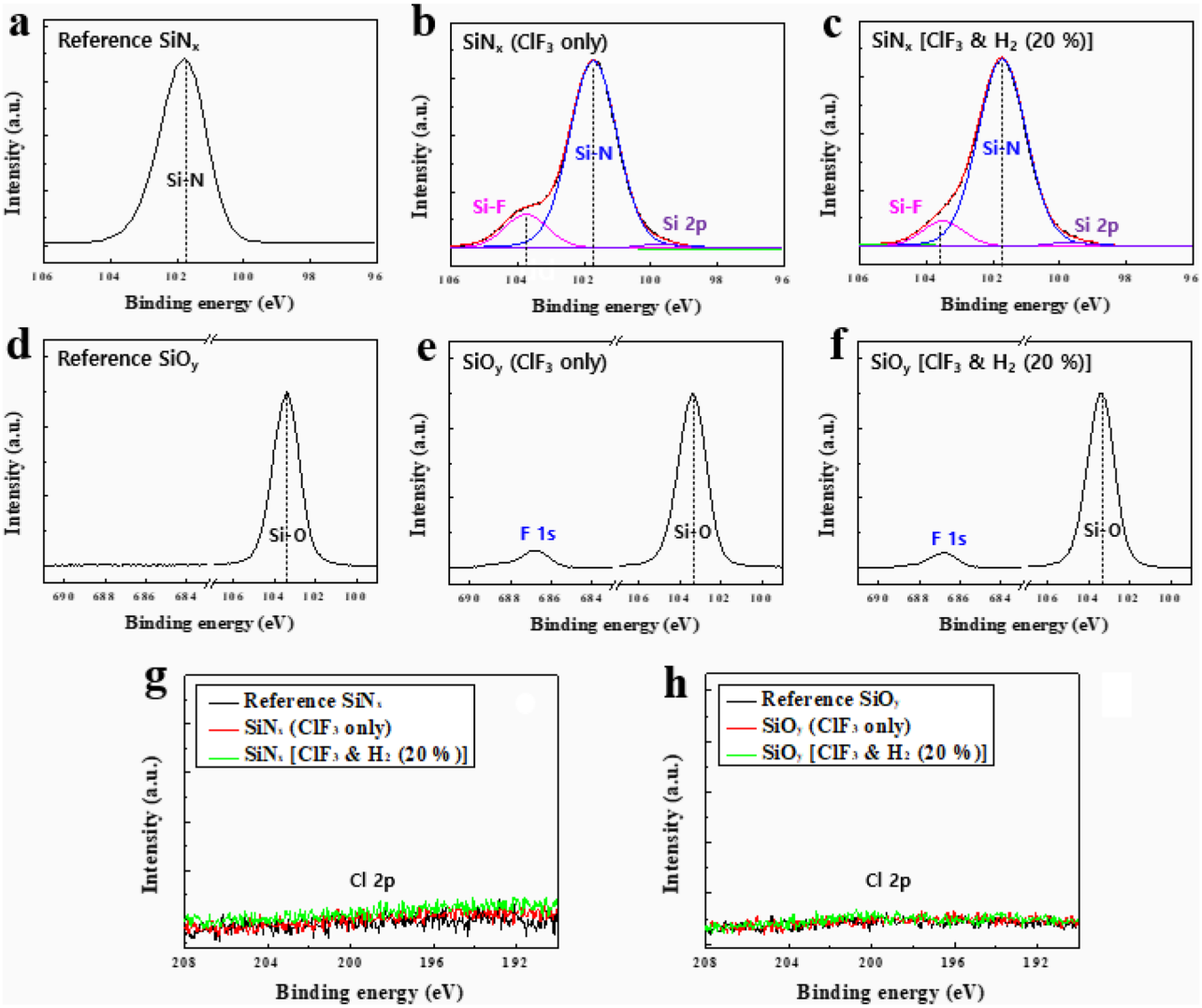

Figure 4. XPS narrow scan (Si 2p) data of SiN_x (**a**-**c**), SiO_y (**d**-**f**), and Cl 2p (**g**, **h**) after etching with a remote ClF_3/H_2 plasma.

Sample	Binding state	B.E. (eV)	FWHM (eV)	% Area	Gaussian %
SiN_x (ClF_3 only)	Si 2p	99.7	1.3	1.6	88.8
	Si–N	101.7	1.7	84.5	87.5
	Si–F	103.6	1.55 (± 0.05)	13.9	85.7
SiN_x [ClF_3 & H_2 (20%)]	Si 2p	99.7	1.3	1.6	88.8
	Si–N	101.7	1.7	88	87.5
	Si–F	103.6	1.55 (± 0.05)	10.4	85.7

Table 1. Parameters related with the curve fitting of silicon nitride (SiN_x) thin films after exposure to the ClF_3 only and ClF_3 & H_2 (20%) plasma.

were etched at the substrate temperature of 25 °C, operating pressure at 200 mTorr, the $ClF_3/H_2/Ar$ flow rates at 200/(0 and 40)/200 sccm, and the rf power at 300 W. As shown in Fig. 4a,d, the reference SiN_x and SiO_y showed only Si–N at 101.7 eV, Si–O at 103.4 eV, respectively. After the etching with ClF_3 plasma, however, significant Si–F bonding (103.6 eV) was formed on the SiN_x surface, presumably due to the bonding of Si with F (Fig. 4b). The Si–F bonding ratio decreases with addition of H_2 (20%) because of the reduction of F in the plasma (Fig. 4c and Table 1). However, no chlorine or Si-Cl bonding (~ 103.3 eV) was observed on the surface of SiN_x even though there were enough Cl radicals in the ClF_3/H_2 plasma as confirmed through OES data in Fig. 3b, presumably, due to the immediate reaction of Si-Cl with F radicals. Meanwhile, as shown in Fig. 4e,f), there was no significant change in F concentration on the SiO_y surface during etching with ClF_3 and ClF_3/H_2 plasma. Also, no noticeable

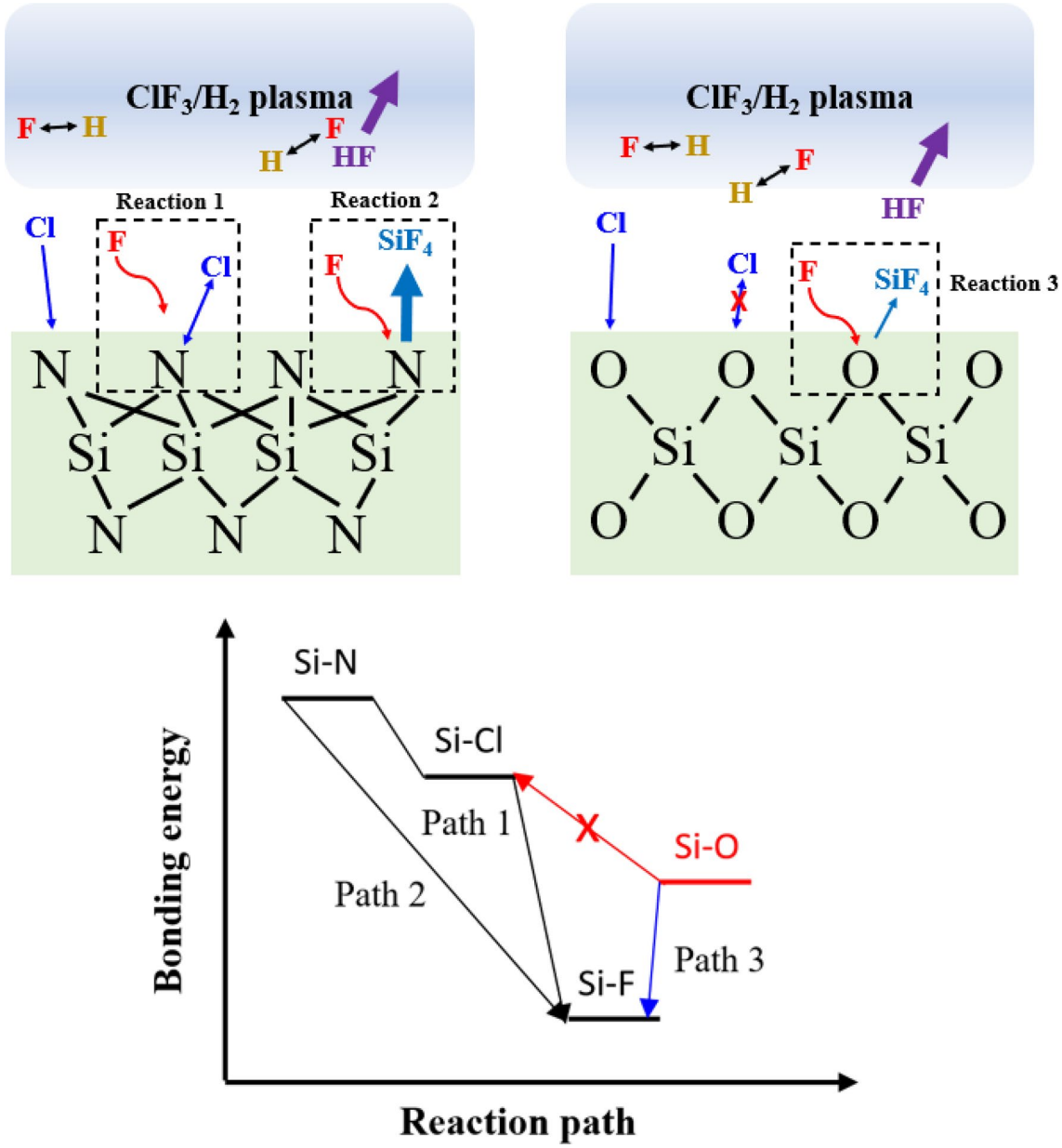

Figure 5. Schematic of chemical reaction of ClF_3/H_2 remote plasma on etching of SiN_x and SiO_y. Possible reaction paths are illustrated.

Si–F bonding formation on the SiO_y surface during the etching with ClF_3 and ClF_3/H_2 plasma was observed from the deconvolution of Si narrow scan data (Si 2p) indicating that most of F is adsorbed on the SiO_y surface after the etching. Furthermore, the amount of F on the SiO_y surface is much lower than that of SiN_x because Si–O bonding is less reactive with F radical compared with SiN_x. As shown in Fig. 4g,h, no chlorine was observed on the surface of both SiN_x and SiO_y even though the chlorine was observed in OES (Fig. 3b). The parameters used for curve fitting of SiN_x is described in Table 1 and the normalized chi-square value for curve fitting was below 0.01. The compositional information of each element can be found in Table S1, supplementary information.

The etching of SiN_x and SiO_y can be explained through the bonding energies of silicon (Si) compounds. Figure 5 shows the etch mechanism of SiN_x and SiO_y under Cl, F radicals. As the bonding energy of Si–F (565 kJ/mol) is higher than those of Si–N (355 kJ/mol) and Si–O (452 kJ/mol)[22], the SiN_x and SiO_y can be etched spontaneously under sufficient F radicals in the plasma although the etching is much active for SiN_x than SiO_y. However, the bonding energy of Si-Cl (381 kJ/mol) is slightly higher than that of Si–N but lower than that of Si–O, and which means the Cl radical can react only with SiN_x and forms Si-Cl bonding. Once the Si–N changes to Si-Cl, Si-Cl can be more easily converted to Si–F by F radicals in the plasma (due to the quick conversion of Si-Cl to Si–F as shown in Fig. 5, no chlorine could be observed on the surfaces of SiN_x and SiO_y during the etching with ClF_3/H_2), then Si–F on SiN_x is removed as a volatile SiF_4 compound. Meanwhile, the addition of H_2 in the ClF_3 plasma reduces the density of F radicals by forming HF in the plasma causing the decreases of

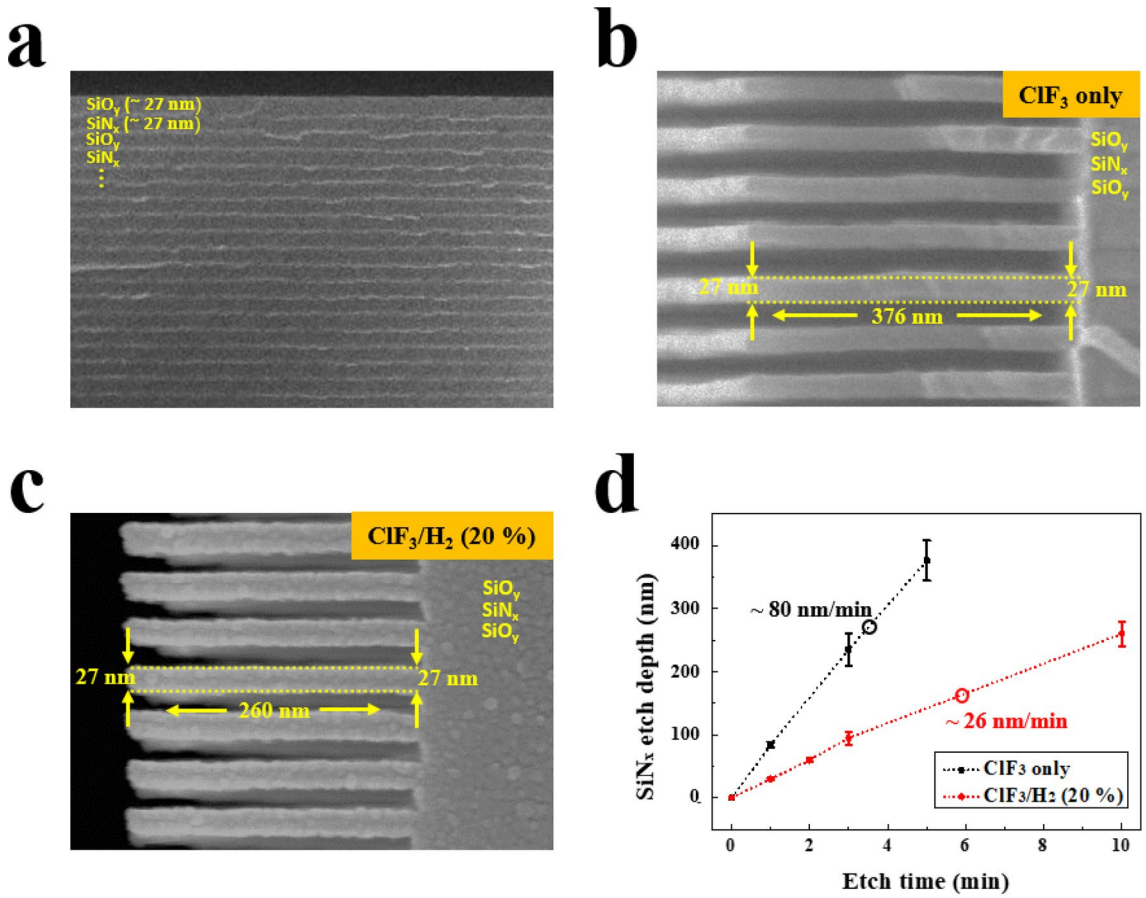

Figure 6. Etch characteristics of ClF_3 only and ClF_3/H_2 (20%) plasma in stacked SiN_x/SiO_y. (**a**) SEM images of reference stacked SiN_x/SiO_y. Etch profile of stacked SiN_x/SiO_y after the etching with (**b**) ClF_3 plasma and (**c**) ClF_3/H_2 (20%) for 5 min and 10 min, respectively. (**d**) Etch depth of SiN_x in the stacked SiN_x/SiO_y with etch time for ClF_3 and ClF_3/H_2 (20%) plasmas.

Si–F formation on the surfaces of SiN_x and SiO_y, and which results in the decrease of etch rates of SiN_x and SiO_y. However, because the concentration of chlorine in the plasma is not significantly affected by the addition of H_2 as confirmed through OES data in Fig. 3c), the etching of SiN_x is decreased more slowly compared to that of SiO_y with increasing H_2 percentage through the conversion of Si-Cl on the surface of SiN_x to Si–F, and which appears to increases the etch selectivity of SiN_x over SiO_y.

Using the etch conditions of ClF_3 and ClF_3/H_2 (20%), stacked layers of SiN_x/SiO_y were etched and the results are shown in Fig. 6. Figure 6a is the reference stack of SiN_x/SiO_y before the etching. Figure 6b,c are the stacked layer of SiN_x/SiO_y after the etching using ClF_3 and ClF_3/H_2 (20%) plasmas for 5 min and 10 min, respectively. As shown in Fig. 6b,c, highly selective etching of SiN_x over SiO_y could be observed for both ClF_3 and ClF_3/H_2 (20%) by showing no noticeable differences in SiO_y thickness along the etch depth. Therefore, it appears that the etch selectivity for the real SiN_x/SiO_y could be higher than that measured with blank wafers. The etch depth with increasing the etch time was also measured and the results are shown in d) for both ClF_3 and ClF_3/H_2 (20%). The measured etch rates of SiN_x with ClF_3 and ClF_3/H_2 remote plasma were 80 and 26 nm/min, respectively, which have similar values with blank samples at the same plasma conditions (Fig. 2a, 3a) because of isotropic etch characteristics of reactive radicals. Furthermore, the etch depth with etch time was linear for both conditions, therefore, no aspect ratio dependent etching was observed. (The process time-dependent etch profiles of SiN_x/SiO_y stacks are shown in figure S2 and S3, supplementary information).

Conclusion

The isotropic and selective etching of SiN_x over SiO_y was studied using ClF_3/H_2 remote plasma with an ICP source. The SiN_x etching using plasma assisted thermal processes showed the highest etch rate as well as the smoothest surface morphology compared with that etched only with thermal etching or plasma etching. The temperature dependent etch characteristics of SiN_x and SiO_y demonstrated a higher activation energy of SiO_y compared that of SiN_x in the ClF_3 remote plasma. Furthermore, the addition of H_2 (20%) to the ClF_3 plasma improved the etch selectivity of SiN_x over SiO_y from 130 to 200 even though the etch rate of SiN_x was decreased from ~ 83 to ~ 23 nm/min. We believe the fast and ultra-high selective SiN_x etching technology can be applied not only to next generation three dimensional NOT-AND type flash memory fabrication process but also to various semiconductor processes where precise etching of SiN_x is required.

Received: 7 December 2021; Accepted: 17 March 2022
Published online: 05 April 2022

References

1. Mirza, M. M. et al. Nanofabrication of high aspect ratio (50:1) sub-10 nm silicon nanowires using inductively coupled plasma etching. *J. Vac. Sci. Technol. B* **30**, 06FF02 (2012).
2. Seo, D., Bae, J. S., Oh, E., Kim, S. & Lim, S. Selective wet etching of Si_3N_4/SiO_2 in phosphoric acid with the addition of fluoride and silicic compounds. *Microelectron. Eng.* **118**, 66–71 (2014).
3. Bassett, D., Printz, W. & Furukawa, T. Etching of silicon nitride in 3D NAND structures. *ECS Trans.* **69**, 159 (2015).
4. Chien, Y. H. C., Hu, C. C. & Yang, C. M. A Design for selective wet etching of Si_3N_4/SiO_2 in phosphoric acid using a single wafer processor. *J. Electrochem. Soc.* **165**, H3187 (2018).
5. Kim, T., Son, C., Park, T. & Lim, S. Oxide regrowth mechanism during silicon nitride etching in vertical 3D NAND structures. *Microelectron. Eng.* **221**, 111191 (2020).
6. Bouchilaoun, M. et al. A Hydrogen Plasma Treatment for Soft and Selective Silicon Nitride Etching. *Phys. Status Solidi (A)* **215**, 1700658 (2018).
7. Chen, L., Xu, L., Li, D. & Lin, B. Mechanism of selective Si_3N_4 etching over SiO_2 in hydrogen-containing fluorocarbon plasma. *Microelectron. Eng.* **86**, 2354–2357 (2009).
8. Lee, S., Oh, J., Lee, K. & Sohn, H. Ultrahigh selective etching of Si_3N_4 films over SiO_2 films for silicon nitride gate spacer etching. *J. Vac. Sci. Technol. B* **28**, 131–137 (2010).
9. Kastenmeier, B. E. E., Matsuo, P. J. & Oehrlein, G. S. Highly selective etching of silicon nitride over silicon and silicon dioxide. *J. Vac. Sci. Technol. A* **17**, 3179–3184 (1999).
10. Ogawa, H., Arai, T., Yanagisawa, M., Ichiki, T. & Horiike, Y. Dry cleaning technology for removal of silicon native oxide employing hot NH_3/NF_3 exposure. *Jpn. J. Appl. Phys.* **41**, 5349 (2002).
11. Volynets, V. *et al.* Highly selective Si3N4/SiO2 etching using an NF3/N2/O2/H2 remote plasma. I. Plasma source and critical fluxes. *J. Vac. Sci. Technol. A* **38**, 023007 (2020).
12. Jung, J. E. *et al.* Highly selective Si3N4/SiO2 etching using an NF3/N2/O2/H2 remote plasma. II. Surface reaction mechanism. *J. Vac. Sci. Technol. A* **38**, 023008 (2020).
13. Kastenmeier, B. E. E., Matsuo, P. J., Oehrlein, G. S. & Langan, J. G. Remote plasma etching of silicon nitride and silicon dioxide using NF_3/O_2 gas mixtures. *J. Vac. Sci. Technol. A* **16**, 2047–2056 (1998).
14. Raju, R., Kudo, D., Kubo, Y., Inaba, T. & Shindo, H. Warming Potential reduction of C_4F_8 using inductively coupled plasma. *Jpn. J. Appl. Phys.* **42**, 280 (2003).
15. Mouri, I. & Hayakawa, S. Application of fluorine-containing gases for cleaning CVD systems in consideration of global environmental problems -1- corrosion-resistance of materials used for CVD systems against ClF_3. *J. Agric. Meteorol.* **52**, 849–852 (1997).
16. Flamm, D. L. Mechanisms of silicon etching in fluorine- and chlorine-containing plasmas. *Pure Appl. Chem.* **62**, 1709–1720 (1990).
17. Seki, T. et al. Angled etching of Si by ClF_3-Ar gas cluster injection. *Jpn. J. Appl. Phys.* **56**, 06HB02 (2017).
18. Yamamoto, H., Seki, T., Matsuo, J., Koike, K. & Kozawa, T. High-aspect-ratio patterning by ClF_3-Ar neutral cluster etching. *Microelectron. Eng.* **141**, 145–149 (2015).
19. Ibbotson, D. E., Mucha, J. A., Flamm, D. L. & Cook, J. M. Plasmaless dry etching of silicon with fluorine-containing compounds. *J. Appl. Phys.* **56**, 2939–2942 (1984).
20. Leinenbach, C., Seidel, H., Fuchs, T., Kronmueller, S. & Laermer, F. A novel sacrificial layer technology based on highly selective etching of silicon-germanium in CLF_3. *IEEE 20th International Conference on Micro Electro Mechanical Systems (MEMS)* 65–68 (2007).
21. Habuka, H. *et al.* Silicon carbide etching using chlorine trifluoride gas. *Jpn. J. App. Phys.* **44**, 1376 (2005).
22. Ibbotson, D. E., Mucha, J. A., Flamm, D. L. & Cook, J. M. Selective interhalogen etching of tantalum compounds and other semiconductor materials. *Appl. Phys. Lett.* **46**, 794–796 (1985).
23. Kim, J. H., Lee, H. J., Joo, J. H. & Whang, K. W. Effect of the radical loss control by the chamber wall heating on the highly selective SiO_2 etching. *Appl. Sci. Converg. Technol.* **5**, 169–174 (1996).
24. Nakayama, D. *et al.* Highly selective silicon nitride etching to Si and SiO_2 for a gate sidewall spacer using a $CF_3I/O_2/H_2$ neutral beam. *J. Phys. D.* **46**, 205203 (2013).
25. Knotter, D. M. & Denteneer, T. D. Etching mechanism of silicon nitride in HF-based solutions. *J. Electrochem. Soc.* **148**, F43 (2001).
26. Tian, F. & Teplyakov, A. V. Silicon Surface Functionalization Targeting Si-N Linkages. *Langmuir* **29**, 13–28 (2013).

Acknowledgements

This research was supported by the MOTIE [Ministry of Trade, Industry & Energy (20003665)], KSRC (Korea Semiconductor Research Consortium) support program for the development of the future semiconductor device, and Samsung Electronics Co., Ltd. (IO201211-08086-01). This research was also supported by the SungKyunKwan University and the BK21 FOUR (Graduate School Innovation) funded by the Ministry of Education (MOE, Korea) and National Research Foundation of Korea (NRF). The authors would like to thank to Wonik IPS for the supply of SiN_x/SiO_y stack wafer and to Wonik Materials for the supply of ClF_3 gas.

Author contributions

G.Y.Y initiated the project. W.O.L., K.H.K. and G.Y.Y. contributed to the experimental design. W.O.L., K.H.K. wrote the main manuscript text. D.S.K., J.W.P. contributed contributed to the experimental setup. H.W.T. carried out OES measurement. Y.J.J., J.E.K. performed plasma processing. All authors reviewed the manuscript.

Competing interests

The authors declare no competing interests.

Additional information

Supplementary Information The online version contains supplementary material available at https://doi.org/10.1038/s41598-022-09252-3.

Correspondence and requests for materials should be addressed to G.Y.